Cardiovascular Engineering and Technology, Vol. 10, No. 1, March 2019 *(© 2018)* pp. 95–111
https://doi.org/10.1007/s13239-018-00394-y

A Novel Pulse Damper for Endothelial Cell Flow Bioreactors

M. M. Alloush,[1] M. Liermann,[1,3] A. Zedan,[2] and G. F. Oweis [1]

[1]Department of Mechanical Engineering, MS Faculty of Engineering and Architecture, American University of Beirut, P.O. Box 11-0236, Beirut, Lebanon; [2]Department of Physiology, Faculty of Medicine, American University of Beirut, P.O. Box 11-0236, Beirut, Lebanon; and [3]Danfoss Power Solutions, Krokamp 35, 24539 Neumünster, Germany

(Received 4 August 2018; accepted 13 November 2018; published online 28 November 2018)

Associate Editor Jonathan Butcher and Ajit P. Yoganathan oversaw the review of this article.

Abstract

Purpose—Peristaltic pumps (PP) are favored in flow bioreactors for their non-contact sterile design. But they produce pulsatile flow, which is consequential for the cultured cells. A novel pulse damper (PD) is reported for pulsatility elimination.

Methods—The PD design was implemented to target static pressure pulsatility and flow rate (velocity) pulsatility from a PP. Damping effectiveness was tested in a macro-scale, closed-loop recirculating bioreactor mimicking the aortic arch at flow rates up to (4 L/min). Time-resolved particle image velocimetry was used to characterize the velocity field. Endothelial cells (EC) were grown in the bioreactor, and subjected to continuous flow for 15 min with or without PD.

Results—The PD was found to be nearly 90% effective at reducing pulsatility. The EC exposed to low PP flow *without PD* exhibited distress signaling in the form of increased ERK1/2 phosphorylation (2.5 folds) when compared to those exposed to the same flow *with PD*. At high pump flow *without PD*, the cells detached and did not survive, while they were perfectly healthy with PD.

Conclusions—Flow pulsatility from PP causes EC distress at low flow and cell detachment at high flow. Elevated temporal shear stress gradient combined with elevated shear stress magnitude at high flow are believed to be the cause of cell detachment and death. The proposed PD design was effective at minimizing the hemodynamic stressors in the pump's output, demonstrably reducing cell distress. Adoption of the proposed PD design in flow bioreactors should improve experimental protocols.

Keywords—Peristaltic roller pump, Pulse damper, Dampener, Pulsatile flow, Endothelial cells, Bioreactor, Shear stress, MAP kinase, Cinema PIV.

Address correspondence to G. F. Oweis, Department of Mechanical Engineering, MS Faculty of Engineering and Architecture, American University of Beirut, P.O. Box 11-0236, Beirut, Lebanon. Electronic mail: goweis@aub.edu.lb

NOMENCLATURE

CCD	Charge coupled device
EC	Endothelial cells
ERK	Extra-cellular signal-regulated kinase
fps	Frames per second
HUVEC	Human umbilical vein endothelial cells
ID	Inner diameter
MAP	Mitogen activated protein
OD	Outer diameter
OSI	Oscillatory shear stress
PD	Pulse damper
PDMS	Polydimethylsiloxane
PIV	Particle image velocimetry
PP	Peristaltic pump
psig	Pound per square inch, gauge
RPM	Revolution per minute

SYMBOLS

f	Flow signal (pressure, flow rate, or shear stress)
$\boldsymbol{p}$	Static pressure
$\boldsymbol{q}$	Flow rate
$\boldsymbol{u}(\boldsymbol{y})$	Flow velocity distribution near the vessel wall
y	Perpendicular distance from the vessel wall
μ	Dynamic viscosity
$\boldsymbol{\tau_w}$	Wall shear stress
$\boldsymbol{\psi}$	Damping effectiveness based on signal standard deviation
ϕ	Damping effectiveness based on signal peak-to-peak
$\mathbf{K}$	Peak-to-peak of a waveform or signal
$\boldsymbol{\sigma}$	Standard deviation of a waveform or signal

Subscripts

D	Damped
U	Un-damped

INTRODUCTION

The heart flow output is pulsatile and is characterized by its pressure waveform and velocity waveform, which are generally different in shape and not time-synchronous. Both pulsatile and steady flow models have been adopted in hemodynamic investigations, with steady flow models being a first step before a follow-up pulsatile study. Pulsatility refers to the temporal variations in *static pressure* (p) and in *flow rate* (q). *Static pressure* is the transmural hemodynamic pressure, i.e. the force per unit area acting perpendicular to a vessel (in the radial direction), and causing wall tensile stresses (in the circumferential direction) associated with vessel dilatation and contraction.[53] Pressure is typically measured *in vitro via* a flush-mounted transducer connected to a wall pressure tap.[41] *Flow rate* derives directly from the cross sectional blood velocity profile, which determines the hemodynamic wall *shear stress* (τ_w). It is desirable to use one pulsatile experimental setup for steady flow investigations too.

Peristaltic or roller pumps have been ubiquitous in hemodynamic investigations, and have been particularly favored in flow bioreactors[16,17,24,37,38,46,54] due to their versatility, ease of use, and non-contact sterile design.[19,21] The user selects a pump speed, and the flow rate is read out from manufacturer lookup tables. From personal observations, it is not uncommon that some users may take this reading at face value and use it with ready to use formulas such as Poiseuille's equation to compute the hemodynamic wall shear stress.[26,49] This approach is not strictly accurate because the roller's squeeze/release positive displacement pump action generates significant pulsatility. The flow rate for a 3-roller commercial pump similar to the one used in this paper can fluctuate by as much as 100% or more. While multiple-roller arrangements reduce the severity of pulsatility, it generally remains significant. Moreover, commercial peristaltic pumps do not replicate the pulsatility in humans. It takes dedicated control algorithms to faithfully mimic the physiological waveform.[3,19,34]

Hemodynamic wall shear stress modulates the biological response of the endothelium,.[8,32,42,44] Its time-averaged component is not the only relevant factor in cellular response, but also the spatial,[14] and temporal variations.[10] The latter has been assigned various measures including shear stress slew rate,[23] oscillatory shear stress,[27] and shear stress temporal gradient.[4,52] Temporal shear stress gradients can stimulate the expression of mitogen activated protein (MAP) kinase ERK1/ERK2,[4,18,52] which are important agents released by the endothelium and involved in angiogenesis and apoptosis. Rapid expression of ERK1/ERK2 is a sign of cell distress and has been associated with the formation of atherosclerosis.[11,39,45,58] Pulsatility from PP induces temporal variations in wall shear stress, which may activate this signaling pathway, and inadvertently contaminate a study's outcomes. Flow pulsatility should thus be well-characterized,[22] or eliminated through effective damping strategy.

The common air gap pulse damper[12,49,51] comprises of a container *partially filled* with liquid. The compliant gas traps and dampens *pressure* pulsatility due to acoustic impedance mismatch at the gas/liquid interface. Gas overpressure is often implemented in industry for relative dampening. The effect of gas/liquid volume ratio is a primary consideration and it was investigated by Deng *et al.*[13] in an open loop flow system at flow rates < 0.03 L/min. Increasing the gaseous volume was found to yield better damping. This concept was implemented by Voyvodic *et al.*[51] in a closed-loop recirculating-flow bioreactor system running at flow rates < 0.03 L/min typical of small arteries. They found that a gaseous volume ratio of 40% was optimal, and noted that damping improved at higher pump speeds. They pointed that PD was most effective when installed at the pump's inlet *and* outlet, which is also in agreement with our investigation.[1,2] Viscous damping plays a significant role in *micro-flow* system as found by Voigt *et al.*[50] at flow rates < 0.04 L/min. Viscous damping is expected to be inconsequential at the *macro-flow* scale and flow rates typical of the great arteries such as in the current investigation.

A pulsatile flow from a peristaltic pump has to be actively damped with regard to its *pressure pulsatility* and to its *velocity (flow rate) pulsatility*. The compliant air gap damper addresses mainly pressure pulsatility, but not velocity (flow momentum) pulsatility, at least not in a direct way. Agitation of the liquid/gas interface created by the incoming flow, transmits as unsteadiness to the outlet flow of the PD. This is a primary cause for bubble entrainment that can contaminate the bioreactor. The effect of bubbles can range from being a nuisance[56] to causing cell poisoning.[27,29] An intentional damping strategy that addresses flow rate (velocity) pulsatility is necessary.

This work presents a novel PD design characterized by an air gap arrangement to dampen pulsatility in the static pressure, and a radial diffuser feature to dampen pulsatility in the flow rate (velocity). Care is given to the flow details to avoid air entrainment and for potent *bubble trapping*. The mechanical *damping effectiveness* is assessed, and its bio-functionality is verified with endothelial cells at flow rates up to 4 L/min.

METHODS

Flow Bioreactor

A closed loop, continuous flow bioreactor system was built to study cultured endothelial cells under steady flow conditions. The bioreactor was a simplified model of the aortic arch and cells were grown on its lumen, as shown in (Figs. 1a and 1b). Design considerations could be found in Refs. 1 and 2. The aortic arch had a 180 degrees planar bend of 35 mm radius of curvature at the inner wall, and a circular cross section flow conduit of 14 mm nominal ID. The dimensions were derived from a typical aorta.[5,7] The model was cast from clear PDMS rubber (RTV 615, Momentive, USA) in two matched coronal halves to provide unobstructed optical path for imaging, and to allow access for cell sampling. The arterial wall at the thinnest point was ~ 10 mm thick, which made for a rigid wall model. Video images confirmed the negligible dilation/contraction motion of the wall under pulsatile flow conditions. A 3-roller peristaltic pump (Model FH100X, Fisher Scientific, USA) fitted with 9.5 mm ID, 14 mm OD silicon tubing (BioPharm #36, Fisher Scientific, USA) drove the flow in a continuous fashion through the endothelial cell bioreactor to maintain sterile conditions. The time-averaged maximum nominal flow rate was 4 L/min the highest pump speed of 400 rpm. Cells were exposed to flow for 15 min during the current experiments. A tube-wrap-around electric heater band (Omegalux, Omega, USA) and a K-type

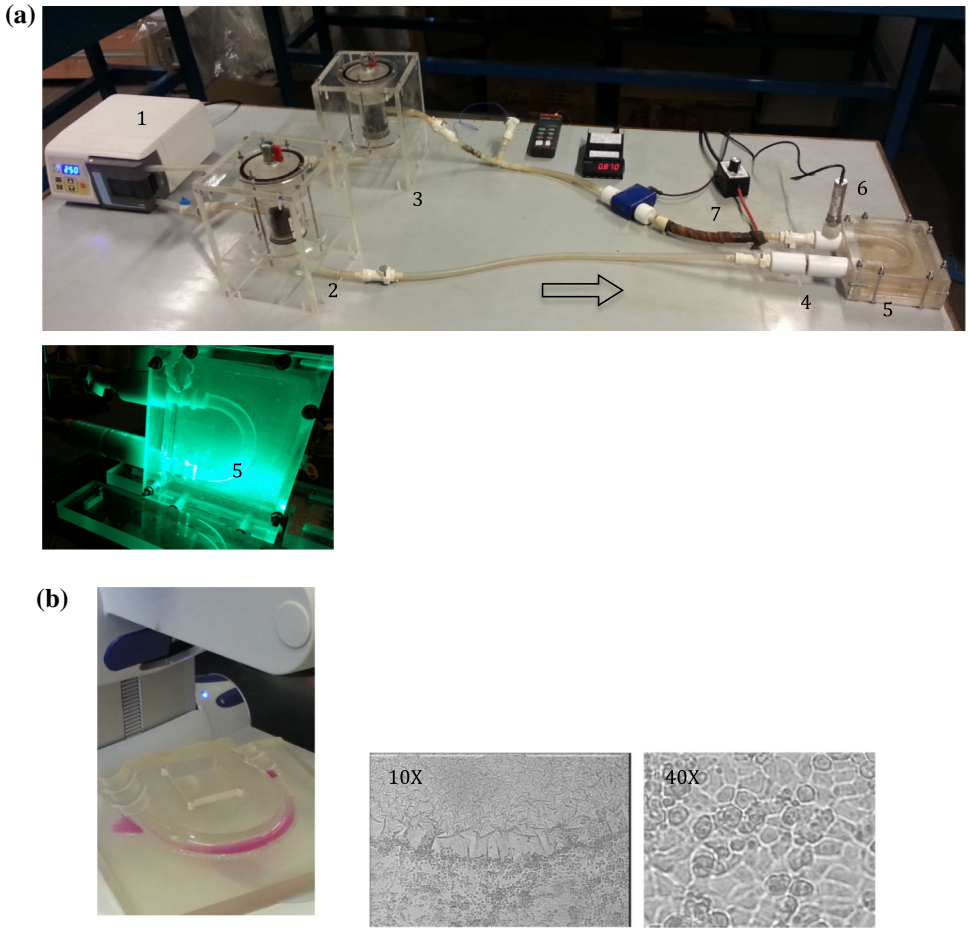

FIGURE 1. (a) Layout of the bioreactor flow loop system: 1. peristaltic pump; 2,3. pulse dampers placed in box fixture; 4. flow straightener and management section; 5. cell culture bioreactor section (aortic arch); 6. pressure transducer; 7. flow temperature control. (b) A picture of one open half of the bioreactor model with endothelial cells and media; a 10 × microscopic image of the cells plated on the model with partial out of focus effect due to the model's curving depth; and a 40 × image of the cells.

thermocouple inserted into the flow were used to maintain the temperature at 37 °C. A 10-diameter long hydrodynamic development section and a flow straightener section conditioned the incoming flow to the bioreactor.

Pulse Damper

The custom-designed PD unit was built in duplicate and installed at the inlet and the outlet of the PP. As illustrated in (Fig. 2), the PD consisted of a cylindrical body nearly half filled with liquid with an air gap on top. A larger diameter top-hat radial diffuser capped the cylinder body, and it consisted of an annular channel formed by two circular discs. The incoming pulsatile flow entered at the eye (center) of the diffuser, and decelerated as it streamed radially to finally seep down the sidewalls of the damper body and collect in a liquid pool at the bottom. A 25:1 decrease in flow speed was achieved across the diffuser by the increase in cross sectional flow area. A very high porosity plastic sponge (mesh) placed in the liquid pool proved effective at arresting any entrained bubbles whilst generating minimal flow frictional loss. The damped flow exited the damper through a low-lying outlet. The damper body was installed in an external rectangular box for good bench-top stability and to minimize shaking and flow unsteadiness by the beating motion

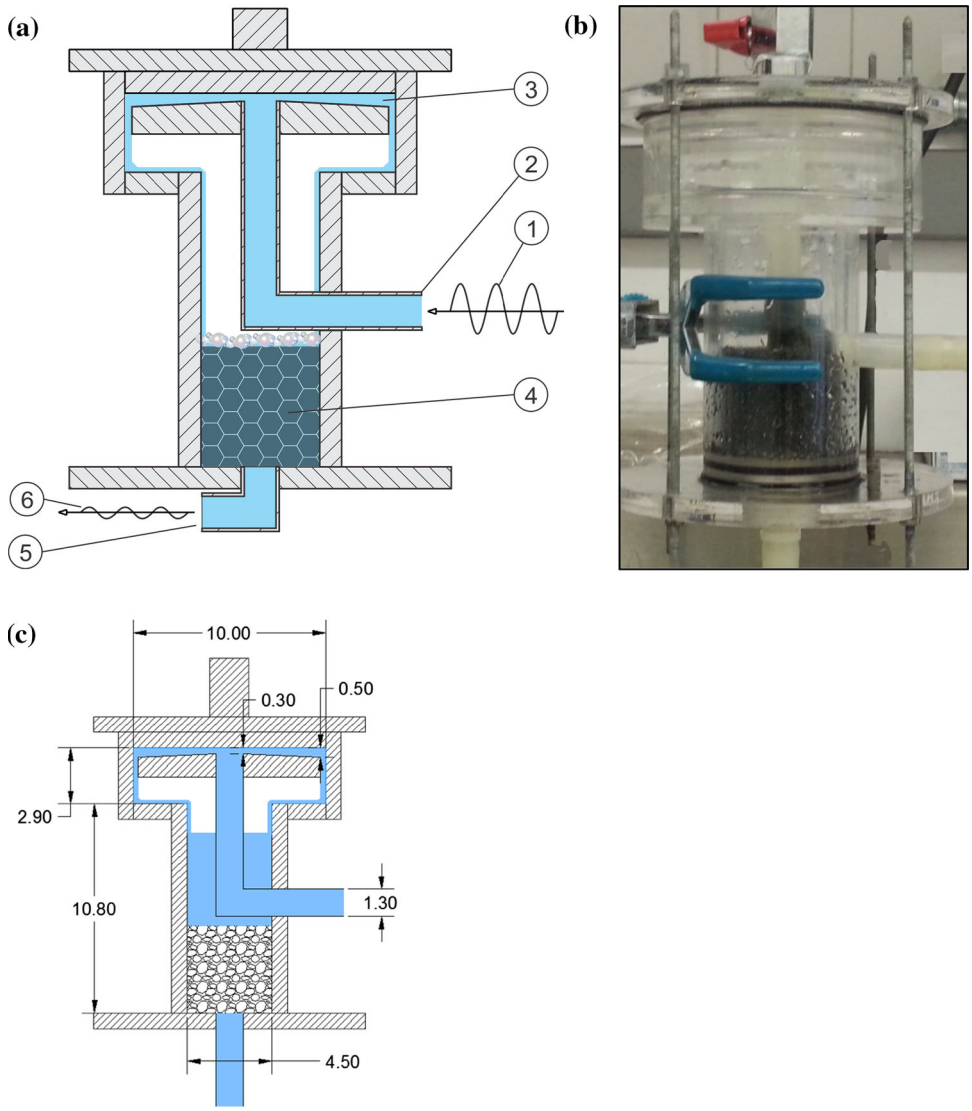

FIGURE 2. (a) Schematic of the pulse dampener design. Liquid pulsatile flow (1) is introduced through the side inlet (2), it flows upwards to the radial diffuser eye, and then decelerates radially outwards through the narrow gap (3). The laminarized flow drains down the sidewalls and collects in the pool at the bottom, which contains a high porosity plastic mesh/sponge to arrest any entrainment bubbles (4), and then exits through the bottom outlet (5) with minimal pulsatility. (b) Picture of the implemented design (external retaining box removed). (c) dimensioned drawing of the PD design (cm).

of the tubing attached to the pump. The pump was placed on a separate bench for further vibration isolation.

Pulse Damper Concept of Operation

The gas volume in the damper body that is in contact with the incoming pulsatile liquid acts as a pressure absorber. When the liquid pressure temporarily increases, the gas absorbs this rise by getting compressed, and thus keeping the pressure stable. When the incoming liquid pressure drops, the compressed gas volume expands to compensate. The gas damping action can be modeled with an isothermal gas expansion process. In it, the product from multiplying the gas pressure by the gas volume remains a constant. The gas volume design concept addresses the pulsatility in pressure. The novelty in our model relates to flow rate pulsation damping, which is done by the radial diffuser element of the design. It works by guiding the pulsatile flow through a conduit of progressively increasing cross sectional area (diffuser). The principle of mass conservation requires the velocity to drop. By designing a large increase in cross sectional area, the velocity is reduced to a negligibly small value with minimal momentum (inertia) and kinetic energy. The kinetic energy is mostly converted to pressure energy, and hence flow rate pulsatility is eliminated.

Flow Characterization in the Bioreactor

A pressure transducer (± 2.5 psig, 1000 sample/s, model PX409, Omega, USA) measured the static pressure at the outlet of the bioreactor. It was installed wall-flush in a straight section a few diameters downstream from the bend. A cinematic particle image velocimetry (PIV) system measured the 2-D velocity distribution near the inlet of the bioreactor in a centerline plane parallel to the plane of the bend. The PIV system consisted of a 3.5 W Argon ion continuous wave laser (Laser Physics, UK), and a Phantom V9.1 CCD camera (Vision Research, USA) framing at around 500 fps at a resolution of 1632 × 1200 pixel (35 mm × 25 mm). The laser beam was formed through cylindrical lenses into ~ 1 mm thick light sheet, which illuminated (5 μm) glass bead flow tracers for the camera to record. A Matlab® based cross correlation PIV software PIVLAB-2000[20] was used to process the particle images to produce 2D flow velocity vector fields. Index of refraction matching was implemented during the PIV measurements between the PDMS model and the working fluid by using a sodium iodide NaI aqueous solution (45% concentration by weight). This minimized refractive distortions in the optical paths of the camera and laser sheet. The average kinematic viscosity of 0.79 m^2/s was almost the same for the NaI solution and the cell culture media, warranting hemodynamic similarity (same Reynolds number Re) between the PIV experiments, and cell culture experiments. The PIV and cellular experiments were run independently, but because of the matched Re, the flow measurements from the former could be extended to the latter. A sample raw PIV image and a processed velocity vector field are shown in (Fig. 3). Also shown is a sample scatter plot of the velocity profile $u(y)$ near the wall of the bioreactor with a linear fit to estimate the wall shear rate. The wall shear stress (τ_w) was computed using $\tau_w = \mu \frac{du}{dy}_{y=0}$, where u is the velocity component parallel to the wall of the bioreactor; y is the perpendicular distance from the wall; $\frac{du}{dy}_{y=0}$ is the shear rate at the wall; and μ is the fluid's dynamic viscosity. Additional measurement details can be found in Ref. 2.

Cell Culture Testing

Human umbilical vein endothelial cells (HUVEC) were cultured in endothelial cell media (PromoCell) at 37 °C and 5% CO_2 in a humidifier incubator.[55] The aortic arch model was opened into two halves to access the lumen, and was coated with collagen to promote cell attachment. The cells were plated on the model and they became confluent 24 h later. The two halves were secured together after excess non-adherent cells were gently washed. The circulatory pump was connected and the cells were exposed to continuous flow at low (50 rpm) or high (400 rpm) pump speeds with or without PD for 15 min. The bioreactor model was opened and the cells were examined near the inlet region where PIV data were acquired. The activation of the stress proteins ERK1/ERK2 was determined with western immunoblotting[55] using an ECL protein detection system (Santa Cruz Biotechnology, Inc., Santa Cruz, CA). The total-ERK (t-ERK) was used for signal normalization.

RESULTS

Time Averaged Flow and Pressure in the Bioreactor

PIV time-averaged flow rate and static pressure measurements with and without the PD installed in the flow loop are shown in (Fig. 4) as a function of the pump rotational speed. The cross sectional velocity profile from PIV was integrated over the aortic vessel

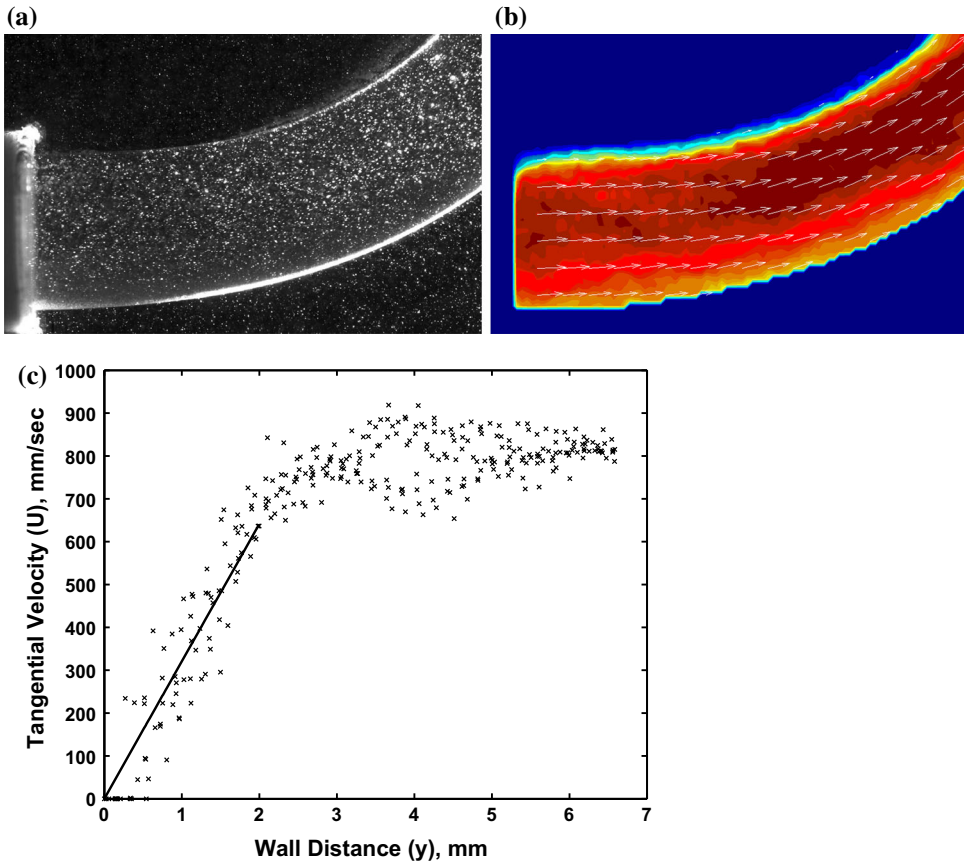

FIGURE 3. (a) A sample raw particle image for PIV taken at the inlet section of the aortic-arch bio-reactor. The illuminating planar laser sheet propagated from the right. Flow was from left to right. For scale, the inner pipe diameter was 13.55 mm; (b) A sample velocity vector field showing velocity magnitude color contours, overlaid with every tenth velocity vector. (c) Scatter plot of the instantaneous wall-parallel velocity as a function of wall-normal distance for the un-damped flow at 400 rpm. A linear fit (shown) is used to compute the wall shear rate. The scatter was obtained by combining a number of PIV data columns covering a ~ 1 cm stream-wise extent to increase the sample size.

section area to obtain the flow rate near the inlet. The time average flow rate, normally tabulated by manufacturers, increased steadily with pump speed. Temporal flow variations due to pulsatility are masked. The installation of the two PD units resulted in about 15% reduction in flow rate at maximum pump speed, due to increased friction losses. The bioreactor's static pressure increased with pump speed at nearly the same rate for the with-PD case (black x) and the without-PD case (grey o), as seen in (Fig. 4). In either case, the increase in pressure from the lowest speed of 50 rpm to the highest speed of 400 rpm was around 5 kPa. This increase in pressure was due to a reduction in the effective tube volume squeezed by the pump rollers with the faster peristaltic action. The plot also shows that the pressure in the damped case was higher than the un-damped case by a constant difference of ~ 8 kPa for all speeds. This difference was a characteristic of the PD dynamics and operation, in which a buildup in the PD gas pressure was related to steadying of the flow and pressure signals downstream.

Transient Startup/Shutdown Performance

The pump speed was manually increased from 0 to 400 rpm in a few seconds, kept for ~ 120 s, and then it was turned off. With PD, an imbalance developed in the liquid levels of the two dampers (initially at equal levels) favoring more liquid in the unit installed at the pump outlet until the levels attained a new steady state. The transient system static pressure rose by about 10 kPa from the resting pressure as seen in (Fig. 5). Without PD, the system's pressure increased, but only by about 4 kPa, and it exhibited substantially higher level of oscillations, of 4 kPa peak-to-peak. When the system was turned off, the static pressure returned to its original level more quickly in the absence of the PD, than in the damped case.

Flow and Pressure Waveforms

Next, the time varying flow and pressure signals in the bioreactor are presented. The frame rate of the

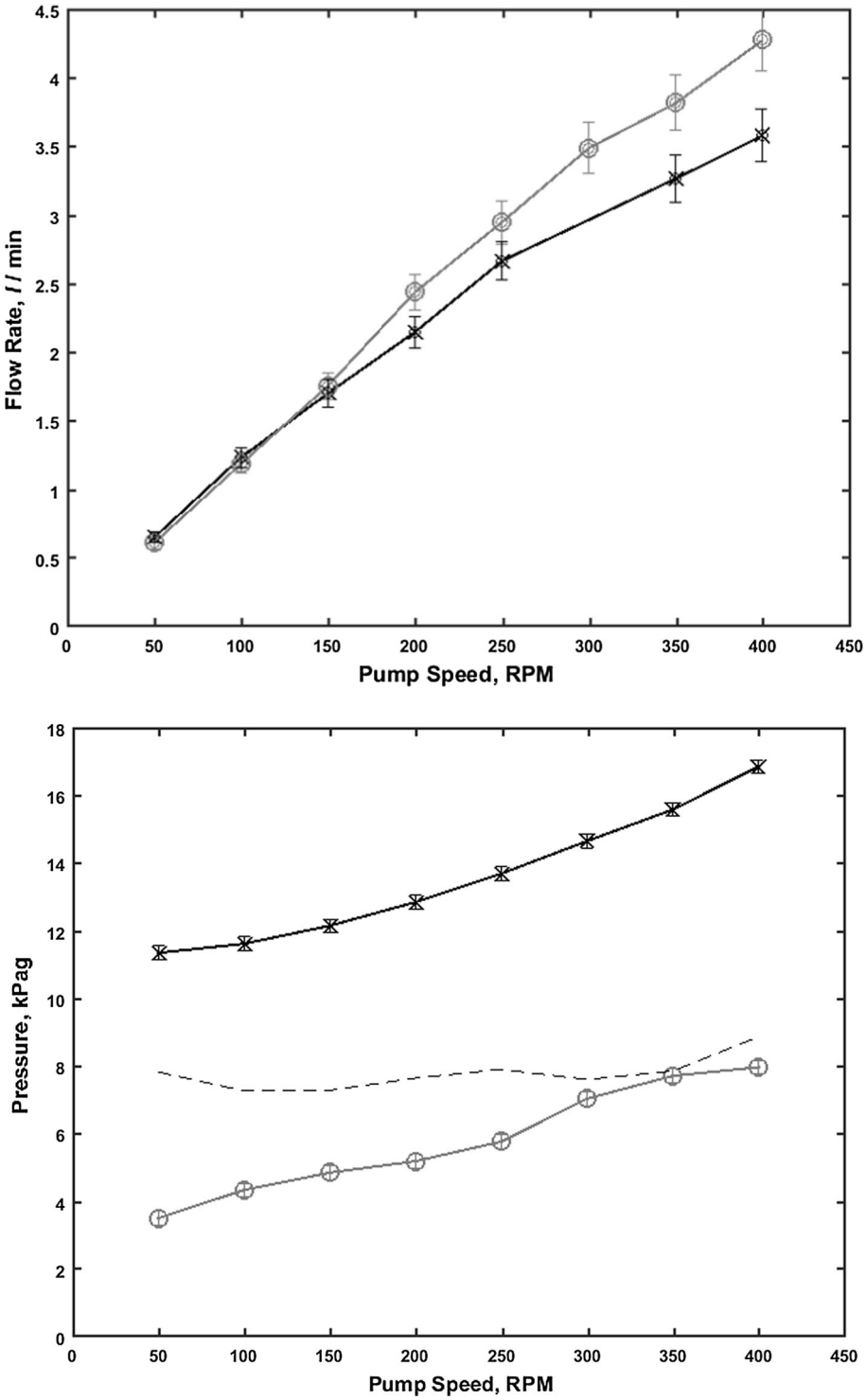

FIGURE 4. Time averaged flow rate, and static pressure in the bioreactor at different pump rotational speeds *with PD* (black x) and *without PD* (gray o). The vertical bars represent the uncertainty in the flow rate and pressure measurements. The error bars for pressure are similar in size to the plot symbols. The dashed line represents the pressure differential between the damped and undamped states.

cinematic PIV system was set between 500 and 1000 fps depending on the pump speed to capture the pulsatile flow waveform. The pressure transducer acquired 1000 samples per second. The 3-roller pump had a maximum speed of 400 rpm, equivalent to a peristaltic pulse frequency of 20 Hz. Figure 6 presents the flow rate

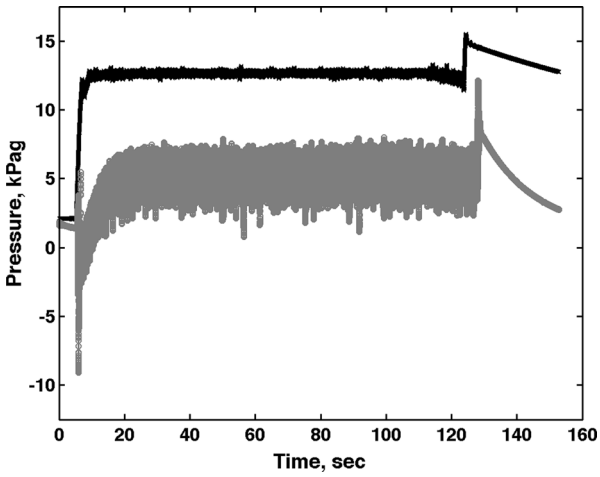

FIGURE 5. Transient behavior of the static pressure signal in the bioreactor during pump start up and shut down *with PD* (black x) and *without PD* (gray o). The pump speed was taken up from 0 to 400 rpm in a few seconds, kept there for 2 min, and then switched off.

waveform for pump speeds from 50 to 400 rpm, for the two cases with and without PD. Signs of higher harmonics can be noted in the un-damped flow as reported previously,[15] which confirms that the flow output of a PP has more to it than the speed dial reading. Flow pulsatility is mostly eliminated by the PD. The static pressure is plotted in (Fig. 7) for the damped and un-damped flow systems. It shows a nearly sinusoidal waveform at all rpms. The mean baseline pressure was higher in the case with the dampers as noted in (Fig. 5).

Wall Shear Stress Waveform

The instantaneous wall shear stress was computed for each PIV realization, and its temporal variations were plotted in (Fig. 8). The signal is relatively noisy, and the uncertainty is expected to be higher than that for pressure or flow rate as evaluated in Ref. 50. The periodic nature due to peristaltic pumping *without PD* is evident at all RPM, while it is diminished to a great degree by the introduction of the PD. Oscillatory shear stress OSI[40] can be used to quantify temporal unsteadiness. Due to the significant forward flow component in our reactor, a modified OSI was computed:

$$\mathrm{OSI} = \left(\frac{\int|\tau - \bar{\tau}|dt}{\int \tau dt}\right) \times 100\%$$

where $\bar{\tau} = \frac{\int \tau dt}{\int dt}$ is the time-average shear stress. OSI is the ratio of the unsteady component to the steady component of the shear stress signal. A 0% indicates the flow is completely steady, and a higher OSI indicates more severe pulsatility. Table 1 summarizes the shear stress characteristics at different speeds including the min, max, time-average, and the OSI. Averaged over the whole speed range of the pump, the max-to-min shear stress ratio is 152% for the damped flow, and 330% for the un-damped flow; i.e. the temporal shear stress gradient in the latter is significantly higher. This is further corroborated by the high ratio of the OSI of the un-damped to the damped flow, which averages to 455% over the pump speed range. This confirms the significant PD effect on the flow, which is related to cell response. There is little effect overall of the PD on the time-average shear stress; the un-damped-to-damped ratio over the speed range is only 108%.

Pulse Damper Effectiveness

Two quantitative pulse damping effectiveness measures (ψ, ϕ) are introduced, based on the standard deviation (σ), and the peak-to-peak (K) of the flow signal (f), respectively. The standard deviation of the time varying flow signal f, is defined as: $\sigma = \sqrt{\frac{\int (f-\bar{f})^2 dt}{\int f dt}}$, with $\bar{f} = \frac{\int f dt}{\int dt}$ being the time-average. The peak-to-peak (K) is the difference between the averaged temporal maxima and the temporal minima of the flow signal: $K = \bar{f}_{max} - \bar{f}_{min}$. The flow signal f can be the pressure (p), the flow rate (q), or the wall shear stress (τ). The effectiveness measures are defined as $\psi = \frac{\sigma_U - \sigma_D}{\sigma_U} \times 100\%$; and $\phi = \frac{K_U - K_D}{K_U} \times 100\%$. The subscripts (D, U) refer to the damped, and un-damped measurements, respectively. Effectiveness quantifies the level of removal of the time varying component (pulsatility) from the flow signal by the two pulse dampers installed on either side of the pump. A damping effectiveness of 0% signifies no alteration of signal pulsatility, while a value of 100% indicates complete elimination of pulsatility (perfect damper). This is plotted in (Fig. 9), which shows effectiveness measures (ϕ, ψ) of (90%, 95%) for pressure, and (85%, 90%) for flow rate, indicating effective damping for this preliminary design. A key factor that could be bettered is to secure the system components in place, particularly, the beating of the flexible tubing directly connected to the pump.

Bubble Trapping Functionality of the PD

Visual monitoring of the PD output indicated no bubbles being entrained near the bottom of the PD or escaping from the low lying outlet. Furthermore, the

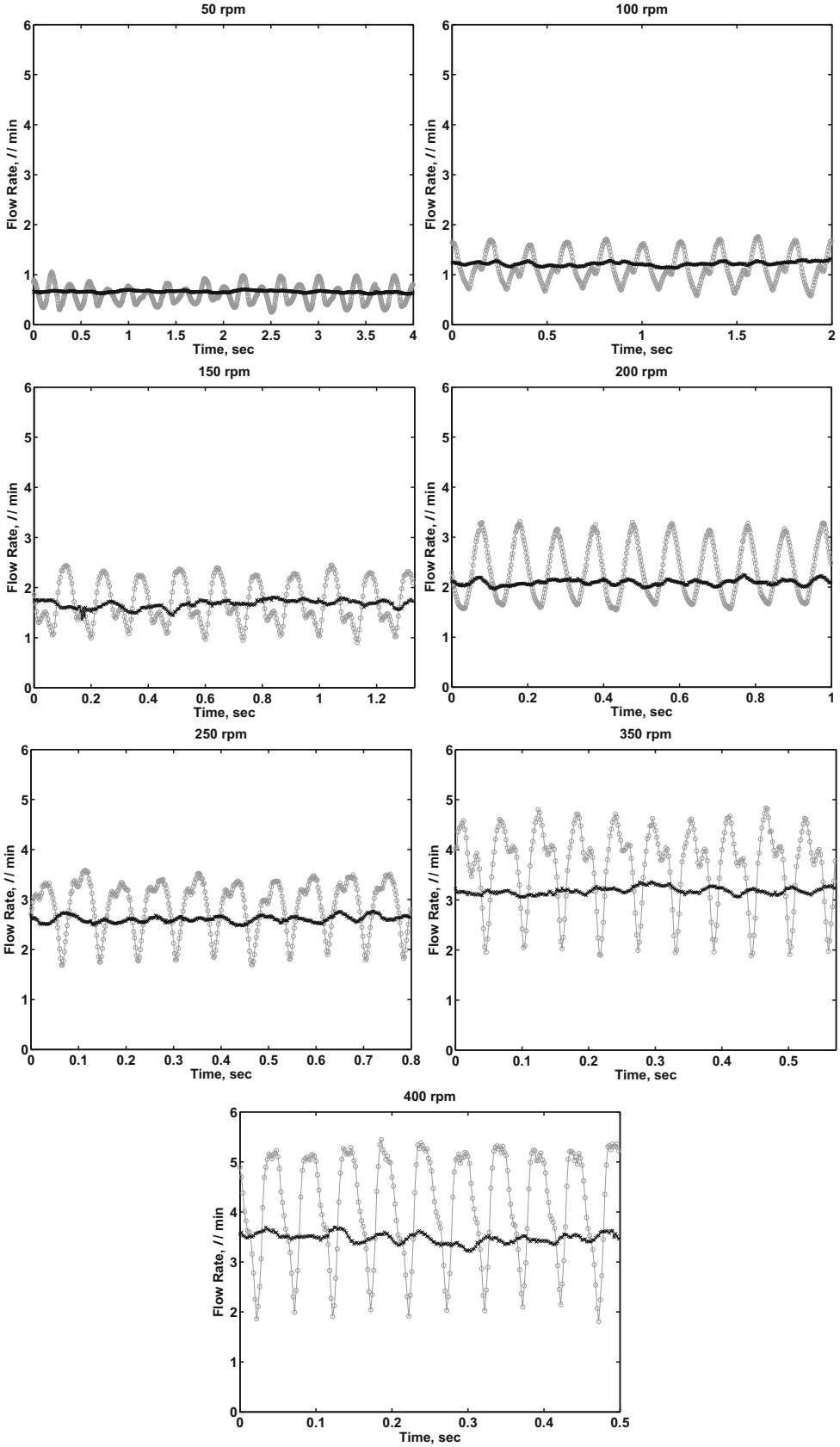

FIGURE 6. Time trace of the PIV-measured flow rate *with PD* (black x) and *without PD* (gray o).

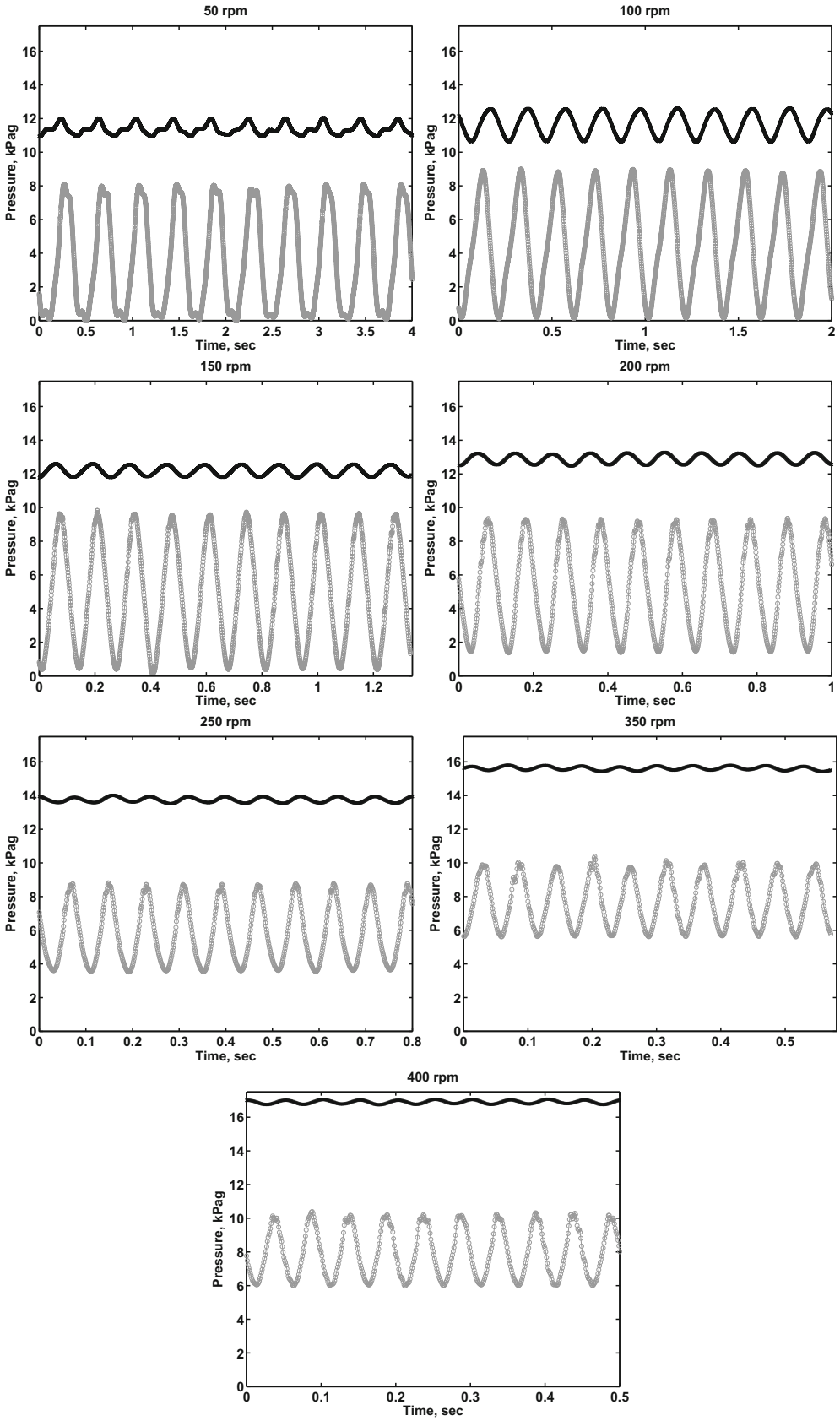

FIGURE 7. Time trace of the static pressure in the bioreactor *with PD* (black x) and *without PD* (gray o).

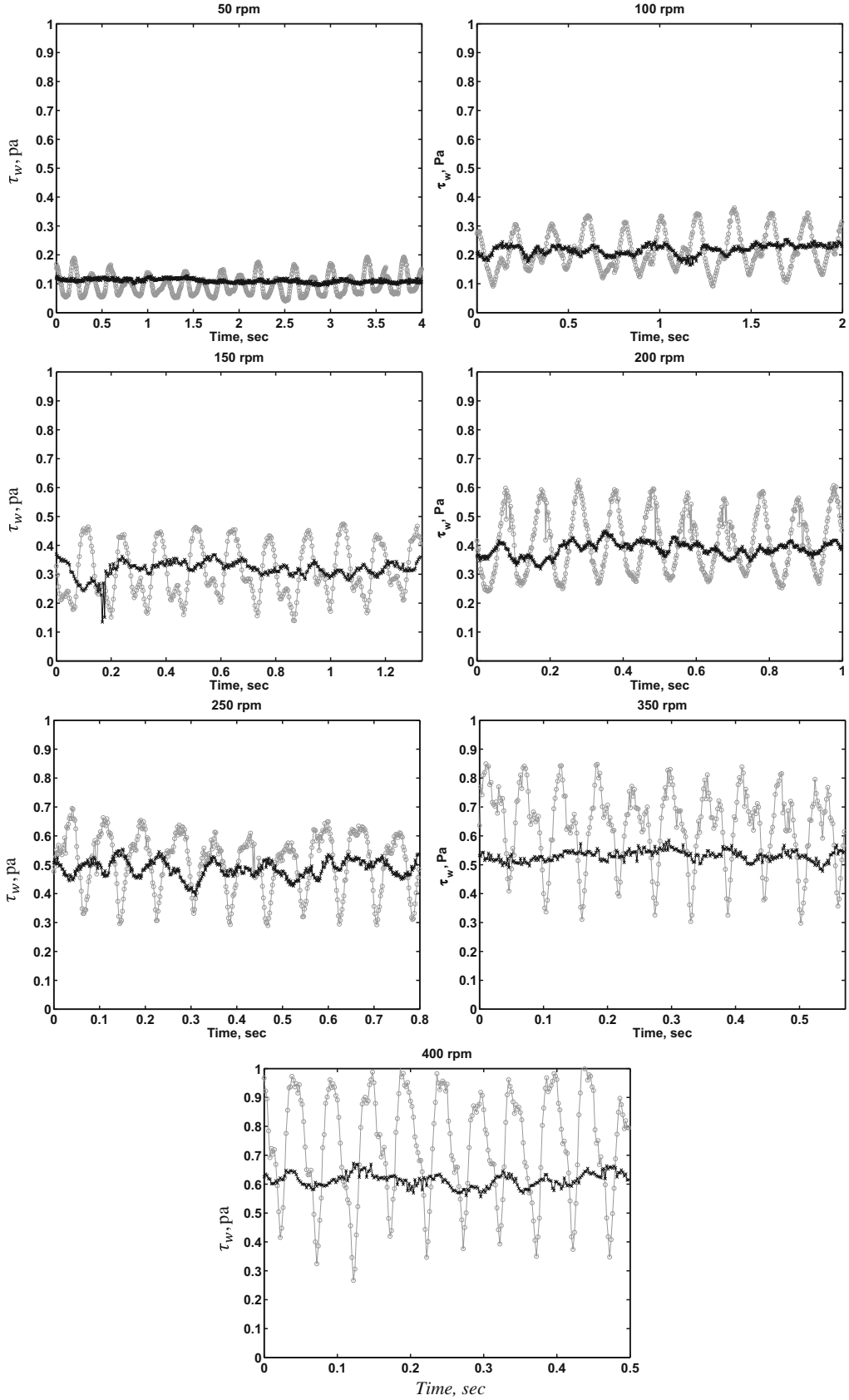

FIGURE 8. Time trace of the wall shear stress near the inlet of the bioreactor *with PD* (black x) and *without PD* (gray o).

TABLE 1. Summary of key pulsatility parameters for wall shear stress in the aortic bioreactor.

	Damped (D)				Undamped (U)				
	τ (Pa)				τ (Pa)				
RPM	Min	Avg	Max	OSI %	Min	Avg	Max	OSI %	OSI ratio (U/D) %
50	0.093	0.112	0.128	4.8	0.040	0.097	0.192	30.4	633
100	0.165	0.218	0.254	6.5	0.092	0.217	0.363	24.9	385
150	0.135	0.318	0.370	6.4	0.139	0.311	0.474	26.0	405
200	0.319	0.387	0.450	5.2	0.241	0.411	0.625	22.7	437
250	0.395	0.487	0.554	4.9	0.290	0.509	0.695	16.3	334
300	0.401	0.463	0.517	4.3	0.304	0.585	0.767	16.1	373
350	0.478	0.531	0.585	2.7	0.298	0.633	0.849	16.9	620
400	0.556	0.614	0.672	3.1	0.267	0.734	1.025	21.8	700

laser assisted PIV images confirmed that no bubbles were present in the bioreactor.

Cell Response to Flow Stimulation

Flow exposure at the low pump speed (50 RPM) without PD significantly activated the ERK1/ERK2 proteins in the endothelial cells compared to those exposed to flow with PD as shown in (Fig. 10). At the high pump speed (400 rpm) without PD, the cells detached from the bioreactor walls and did not survive. They were perfectly healthy, however, with PD. The (OSI_U/OSI_D) ratio (without PD/with PD) was 633 and 700%, at 50 and 400 RPM, respectively. The temporal shear stress gradient is thus much higher without damping and is the possible cause for the increase in ERK expression. When this is also combined with high shear stress at 400 rpm, cell detachment would result. The PD significantly minimized the oscillatory shear stress index and temporal shear stress gradient and significantly affected cell signaling at low RPM and cell viability at high RPM.

SUMMARY AND CONCLUSIONS

The current work highlighted the pulsatile nature of the flow produced by a commercial peristaltic pump and the implications for EC cultures. A novel radial-diffuser PD was shown to be ~ 90% effective at eliminating pulsatility. Improvements in effectiveness are possible through design optimization, and by paying special attention to overall vibration transmission through the different components of the setup. The PD was easy to clean and sterilize, and it demonstrated excellent bubble trapping functionality. PD implementation at the pump's inlet *and* outlet was found necessary, as reported also in Ref. 51. Individual flow characterization of the bioreactor was necessary as has been noted in Refs. [28] and [50].

At the low speed of 50 rpm, it was found that PD decreased ERK1/ERK2 activation associated with cell distress and cardiovascular risk factors.[11,18,45,58] This is consistent with the conclusions of Li *et al.*[33] that high flow pulsatility induces acute endothelial inflammation. Cells exposed to the high pump speed of 400 RPM *without* PD detached from the lumen of the bioreactor and did not survive. Yet, these cells exposed to the same pump speed but *with damping* remained attached and viable. This is primarily attributed to a combination of high temporal shear stress gradient, and a high shear stress magnitude. Implementation of effective PD should improve experimental protocols in endothelial cell flow bioreactors. The design can be replicated by researchers for use with peristaltic pumps at large flow rates and hopefully advanced by commercial developers into a commercially available product.

LIMITATIONS

The goal of this study was to generate a steady flow out of the pulsatility coming out from the PP, at flow rate and vessel size typical of the great arteries. Indeed, cardiovascular blood flow is pulsatile, and thus using pulse damping and steady flow conditions should be limited to studies where a steady flow assumption is justified. This is particularly so in subjects where vessel walls are nearly rigid such as hypertensive old-aged subjects with developed aortic calcification and stiffening.[9,31,36,48] Flow steadiness and wall rigidity are

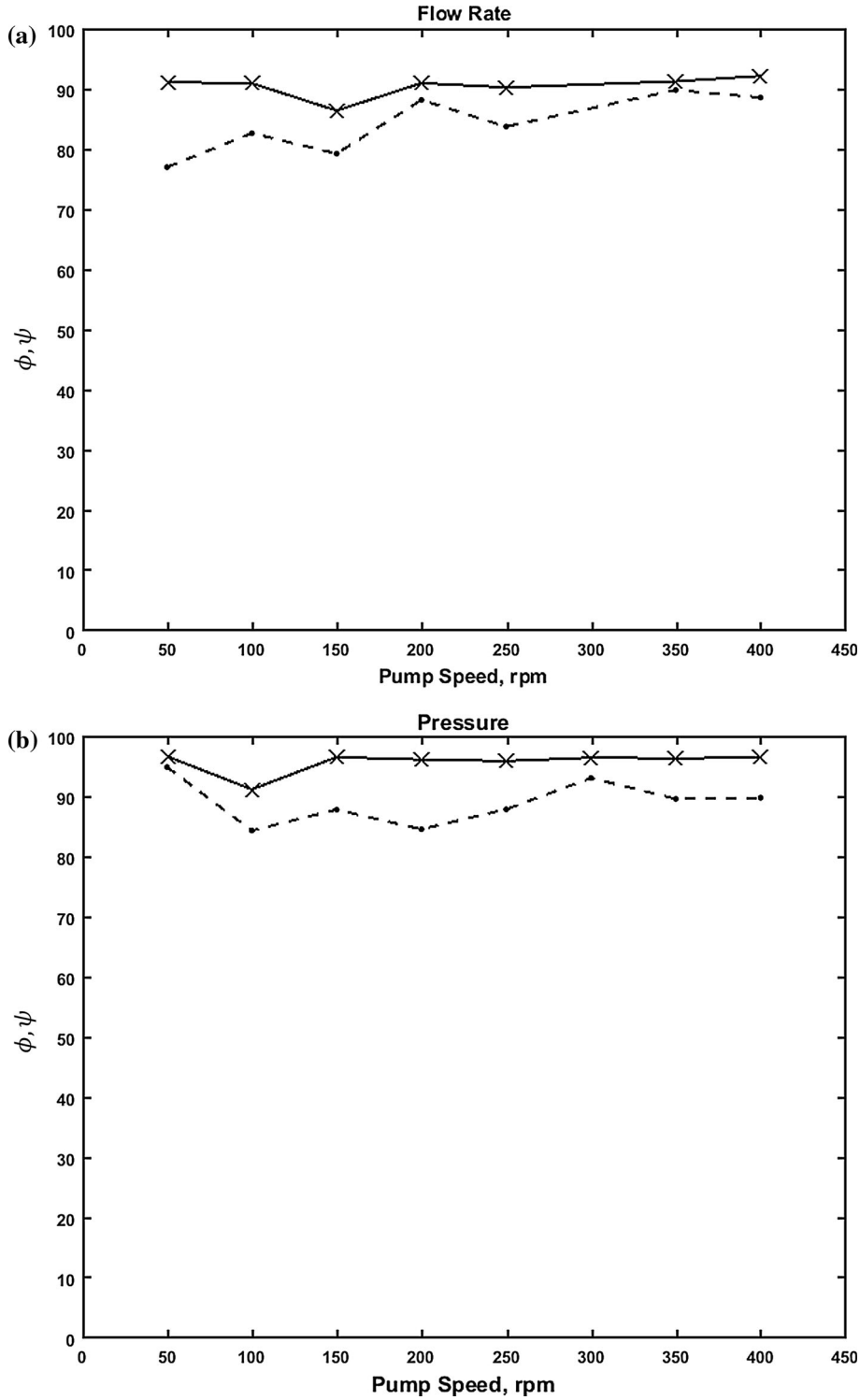

FIGURE 9. Effectiveness of PD at suppressing pulsatility in (a) flow rate; (b) pressure; and (c) shear stress. Two effectiveness measures are reported ψ (solid line) and ϕ (dashed line).

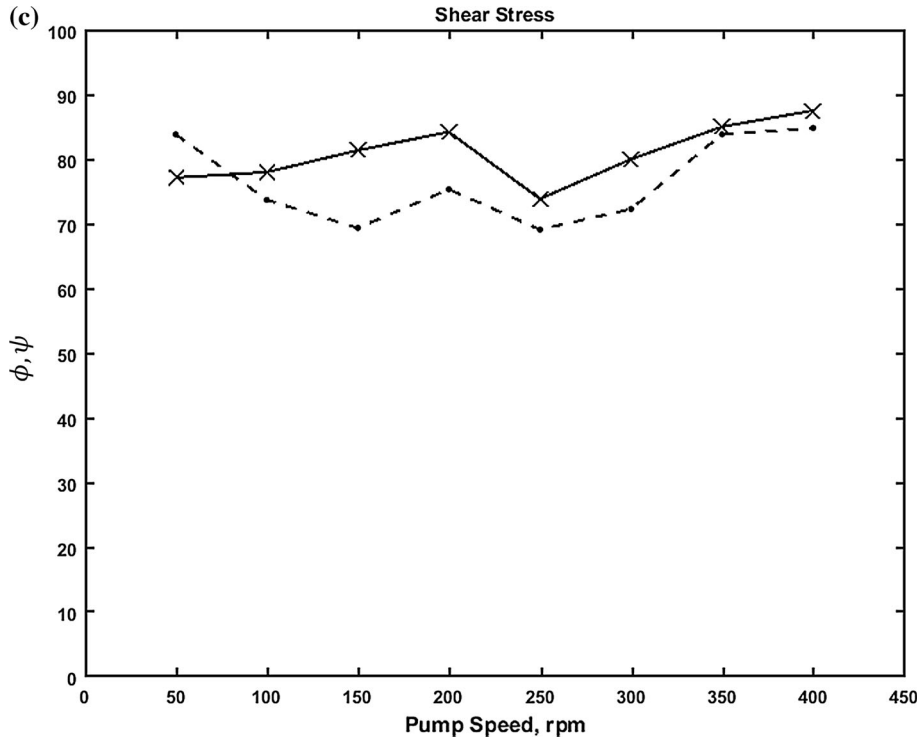

FIGURE 9. continued

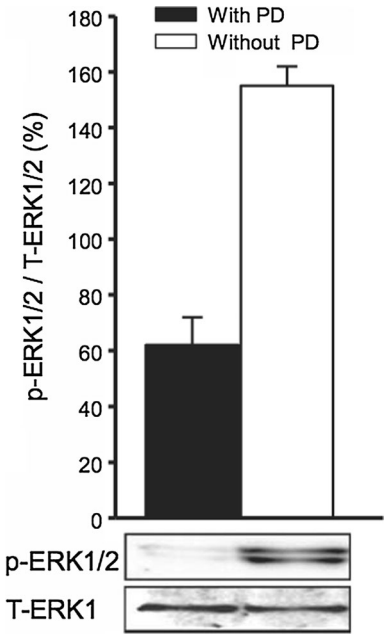

FIGURE 10. Expression of ERK1/ERK2 activation in the endothelial cells after exposure to 15 min flow with or without PD at 50 RPM pump speed. Western blot densitometry scans were normalized by the total-ERK (t-ERK). At 400 RPM, this type of analysis was not possible due to cell detachment in the flow *without PD.*

conjugated because the effect of wall compliance on the flow velocity field is not critical,[6] though it plays a crucial role in pressure pulse propagation. Hemodynamic simulations and MRI measurements showed that flow patterns in rigid models and in compliant models were comparable.[25,30,43] It is typical that the steady flow assumption is used in aortic studies[35,47,57] as a pre-sequel to pulsatile flow studies.

ELECTRONIC SUPPLEMENTARY MATERIAL

The online version of this article (https://doi.org/10.1007/s13239-018-00394-y) contains supplementary material, which is available to authorized users.

ACKNOWLEDGMENTS

Casting molds for the arched bioreactor model were produced *via* CNC machining by J. Nassif and J. Zoullikian. GFO thanks Prof. SL Ceccio from U. Michigan for hosting his sabbatical which made the production of this manuscript possible.

FUNDING

This work was supported by the American University of Beirut through the Faculty of Engineering and Architecture (Dar-Shair Grant), and the Faculty of Medicine (F. Jabre Grant).

CONFLICT OF INTEREST

M.M. Alloush declares that he has no conflict of interest. M. Liermann declares that he has no conflict of interest. A Zedan declares that he has no conflict of interest. G.F. Oweis declares that he has no conflict of interest.

ETHICAL APPROVAL

No human studies were carried out by the authors for this article. No animal studies were carried out by the authors for this article. The HUVEC culture used in this study was obtained commercially.

REFERENCES

[1]Alloush, M. M., G. F. Oweis, R. Nasr, and A. Zeidan. An aortic arch flow loop for the study of hemodynamic-induced endothelial cell injury and inflammation. In: 2014 Middle East Conference on Biomedical Engineering (MECBME), (pp. 67–70), 2014.

[2]Alloush M. M., G. F. Oweis, R. Nasr, and A. Zeidan. Flow Measurements in a Matched-Index-of-Refraction Aortic Arch Model for Endothelial Cell Culture. In: ASME 2014 4th Joint US-European Fluids Engineering Division Summer Meeting. American Society of Mechanical Engineers, 2014.

[3]Asmar, E., G. Bejjani, R. Chamoun, J. Hachem, G. Oweis, and M. Liermann. Experimental Study on Active Pneumatic Damping of Pulsatile Flow Delivered From Peristaltic Pump. In: ASME/BATH 2017 Symposium on Fluid Power and Motion Control, pp. V001T01A066.

[4]Bao, X., C. B. Clark, and J. A. Frangos. Temporal gradient in shear-induced signaling pathway: involvement of MAP kinase, c-fos, and connexin43. *Am. J. Physiol.-Heart Circ. Physiol.* 278(5):H1598–H1605, 2000.

[5]Beller, C. J., *et al*. Role of aortic root motion in the pathogenesis of aortic dissection. *Circulation* 109.6:763–769, 2004.

[6]Berger, S. A., L. Talbot, and L. S. Yao. Flow in curved pipes. *Annu. Rev. Fluid Mech.* 15(1):461–512, 1983.

[7]Borsa, J. J., E. K. Hoffer, R. Karmy-Jones, A. B. Fontaine, R. D. Bloch, J. K. Yoon, C. R. So, M. H. Meissner, and S. Demirer. Angiographic description of blunt traumatic injuries to the thoracic aorta with specific relevance to endograft repair. *J. Endovasc. Ther.* 9(Suppl 2):II-84–II-91, 2002.

[8]Carrisoza-Gaytan, R., Y. Liu, D. Flores, C. Else, H. G. Lee, G. Rhodes, R. M. Sandoval, T. R. Kleyman, F. Y. Lee, B. Molitoris, L. M. Satlin, and R. Rohatgi. Effects of biomechanical forces on signaling in the cortical collecting duct (CCD). *Am. J. Physiol. Renal. Physiol.* 307(2):F195–F204, 2014.

[9]Cavalcante, J. L., J. A. C. Lima, A. Redheuil, and M. H. Al-Mallah. Aortic stiffness: current understanding and future directions. *J. Am. Coll. Cardiol.* 57(14):1511–1522, 2011.

[10]Chiu, J. J., and S. Chien. Effects of disturbed flow on vascular endothelium: pathophysiological basis and clinical perspectives. *Physiol. Rev.* 91(1):327–387, 2011.

[11]Davis, R. J. The mitogen-activated protein kinase signal transduction pathway. *J. Biol. Chem.* 268:14553–14556, 1993.

[12]Dekker, R. J., J. V. van Thienen, J. Rohlena, S. C. de Jager, Y. W. Elderkamp, J. Seppen, and A. J. Horrevoets. Endothelial KLF2 links local arterial shear stress levels to the expression of vascular tone-regulating genes. *Am. J. Pathol.* 167(2):609–618, 2005.

[13]Deng, R., Y. Cheng, and C. H. Wang. Experiments and simulation on a pulse dampener system for stabilizing liquid flow. *Chem. Eng. J.* 210:136–142, 2012.

[14]DePaola, N., M. A. Gimbrone, P. F. Davies, and C. F. Dewey. Vascular endothelium responds to fluid shear stress gradients. *Arterioscler. Thromb. Vasc. Biol.* 12(11):1254–1257, 1992.

[15]Dougherty, F. C., F. M. Donovan, Jr, and M. I. Townsley. Harmonic analysis of perfusion pumps. *J. Biomech. Eng.* 125(6):814–822, 2003.

[16]Dudash, L. A., F. Kligman, S. M. Sarett, K. Kottke-Marchant, and R. E. Marchant. Endothelial cell attachment and shear response on biomimetic polymer-coated vascular grafts. *J. Biomed. Mater. Res. Part A* 100(8):2204–2210, 2012.

[17]Estrada, R., G. A. Giridharan, M. D. Nguyen, T. J. Roussel, M. Shakeri, V. Parichehreh, and P. Sethu. Endothelial cell culture model for replication of physiological profiles of pressure, flow, stretch, and shear stress in vitro. *Anal. Chem.* 83(8):3170–3177, 2011.

[18]Ha, C. H., S. Kim, J. Chung, S. H. An, and K. Kwon. Extracorporeal shock wave stimulates expression of the angiogenic genes via mechanosensory complex in endothelial cells: mimetic effect of fluid shear stress in endothelial cells. *Int. J. Cardiol.* 168(4):4168–4177, 2013.

[19]Hahn, M. S., M. K. McHale, E. Wang, R. H. Schmedlen, and J. L. West. Physiologic pulsatile flow bioreactor conditioning of poly (ethylene glycol)-based tissue engineered vascular grafts. *Ann. Biomed. Eng.* 35(2):190–200, 2007.

[20]Han, D., and M. G. Mungal. Simultaneous measurements of velocity and CH distributions. Part 1: jet flames in coflow. *Combust Flame* 132:565–590, 2003.

[21]Herricks, T., K. B. Seydel, G. Turner, M. Molyneux, R. Heyderman, T. Taylor, and P. K. Rathod. A microfluidic system to study cytoadhesion of Plasmodium falciparum infected erythrocytes to primary brain microvascularendothelial cells. *Lab Chip* 11(17):2994–3000, 2011.

[22]Hoenicka, M., L. Wiedemann, T. Puehler, S. Hirt, D. E. Birnbaum, and C. Schmid. Effects of shear forces and pressure on blood vessel function and metabolism in a perfusion bioreactor. *Ann. Biomed. Eng.* 38(12):3706–3723, 2010.

[23]Hsiai, T. K., S. K. Cho, H. M. Honda, S. Hama, M. Navab, L. L. Demer, and C. M. Ho. Endothelial cell dynamics under pulsating flows: significance of high versus low shear stress slew rates ($\partial \tau/\partial t$). *Ann. Biomed. Eng.* 30(5):646–656, 2002.

[24]Ishibazawa, A., T. Nagaoka, T. Takahashi, K. Yamamoto, A. Kamiya, J. Ando, and A. Yoshida. Effects of shear stress on the gene expressions of endothelial nitric oxide synthase, endothelin-1, and thrombomodulin in human retinal microvascular endothelial cells. *Invest. Ophthalmol. Vis. Sci.* 52(11):8496–8504, 2011.
[25]Jin, S., J. Oshinski, and D. P. Giddens. Effects of wall motion and compliance on flow patterns in the ascending aorta. *J. Biomech. Eng.* 125(3):347–354, 2003.
[26]Kang, H., Y. Fan, and X. Deng. Vascular smooth muscle cell glycocalyx modulates shear-induced proliferation, migration, and NO production responses. *Am. J. Physiol.-Heart. Circ. Physiol.* 300(1):H76–H83, 2010.
[27]Keynton, R. S., M. M. Evancho, R. L. Sims, N. V. Rodway, A. Gobin, and S. E. Rittgers. Intimal hyperplasia and wall shear in arterial bypass graft distal anastomoses: an in vivo model study. *J. Biomech. Eng.* 123(5):464–473, 2001.
[28]Kinney, M. A., C. Y. Sargent, and T. C. McDevitt. The multiparametric effects of hydrodynamic environments on stem cell culture. *Tissue Eng. Part B* 17(4):249–262, 2011.
[29]Kopsachilis, N., K. T. Tsaousis, I. T. Tsinopoulos, and U. Welge-Luessen. Air toxicity for primary human-cultured corneal endothelial cells: an in vitro model. *Cornea* 32(4):e31–e35, 2013.
[30]Lantz, J., J. Renner, and M. Karlsson. Wall shear stress in a subject specific human aorta—influence of fluid-structure interaction. *Int. J. Appl. Mech.* 3(04):759–778, 2011.
[31]Lee, H. Y., and O. Byung-Hee. Aging and arterial stiffness. *Circ. J.* 74(11):2257–2262, 2010.
[32]Lee, E. J., and L. E. Niklason. A novel flow bioreactor for in vitro microvascularization. *Tissue Eng. Part C* 16(5):1191–1200, 2010.
[33]Li, M., Y. Tan, K. R. Stenmark, and W. Tan. High pulsatility flow induces acute endothelial inflammation through overpolarizing cells to activate NF-κB. *Cardiovasc. Eng. Technol.* 4(1):26–38, 2013.
[34]Liermann, M. Active pneumatic pulsation damper for peristaltic pump flow loops. In: BATH/ASME 2016 Symposium on Fluid Power and Motion Control, p. V001T01A005.
[35]Liu, X., P. Fang, Y. Fan, X. Deng, D. Li, and S. Li. A numerical study on the flow of blood and the transport of LDL in the human aorta: the physiological significance of the helical flow in the aortic arch. *Am. J. Physiol.-Heart Circ. Physiol.* 297(1):H163–H170, 2009.
[36]London, G. M., and A. P. Guerin. Influence of arterial pulse and reflected waves on blood pressure and cardiac function. *Am. Heart J.* 138(3):S220–S224, 1999.
[37]Lu, L., M. Mende, X. Yang, H. F. Körber, H. J. Schnittler, S. Weinert, J. Heubach, C. Werner, and U. Ravens. Design and validation of a bioreactor for simulating the cardiac niche: a system incorporating cyclic stretch, electrical stimulation, and constant perfusion. *Tissue Eng. Part A* 19(3–4):403–414, 2012.
[38]Mahler, G. J., C. M. Frendl, Q. Cao, and J. T. Butcher. Effects of shear stress pattern and magnitude on mesenchymal transformation and invasion of aortic valve endothelial cells. *Biotechnol. Bioeng.* 111(11):2326–2337, 2014.
[39]Mebratu, Y., and Y. Tesfaigzi. How ERK1/2 activation controls cell proliferation and cell death: is subcellular localization the answer? *Cell cycle* 8(8):1168–1175, 2009.
[40]Nordgaard, H., A. Swillens, D. Nordhaug, I. Kirkeby-Garstad, D. Van Loo, N. Vitale, P. Segers, R. Haaverstad, and L. Lovstakken. Impact of competitive flow on wall shear stress in coronary surgery: computational fluid dynamics of a LIMA–LAD model. *Cardiovasc. Res.* 88(3):512–519, 2010.
[41]Peattie, R. A., E. Golden, R. S. Nomoto, C. M. Margossian, F. Q. Pancheri, E. S. Edgar, M. D. Iafrati, and A. L. Dorfmann. A technique for comparing wall pressure distributions in steady flow through rigid versus flexible patient-based abdominal aortic aneurysm phantoms. *Exp. Tech.* 40(4):1187–1201, 2016.
[42]Pedroso, P. D., B. L. Hershey, W. Holman, R. Venugopalan, and A. S. Anayiotos. The hemodynamic effects of compliance, bulging, and curvature in a saphenous vein coronary artery bypass graft model. *Technol. Health Care* 11(6):443–455, 2002.
[43]Reymond, P., P. Crosetto, S. Deparis, A. Quarteroni, and N. Stergiopulos. Physiological simulation of blood flow in the aorta: comparison of hemodynamic indices as predicted by 3-D FSI, 3-D rigid wall and 1-D models. *Med. Eng. Phys.* 35(6):784–791, 2013.
[44]Riquelme, M. A., S. Burra, R. Kar, P. D. Lampe, and J. X. Jiang. MAPK Activated by Prostaglandin E2 Phosphorylates Connexin 43 and Closes Osteocytic Hemichannels in Response to Continuous Flow Shear Stress. *J Biol Chem*; jbc.M115.683417, 2015.
[45]Seger, R., and E. G. Krebs. The MAPK signaling cascade. *FASEB J.* 9:726–735, 1995.
[46]Siddharthan, V., Y. V. Kim, S. Liu, and K. S. Kim. Human astrocytes/astrocyte-conditioned medium and shear stress enhance the barrier properties of human brain microvascular endothelial cells. *Brain Res.* 1147:39–50, 2007.
[47]Stevens, M. C., F. M. Callaghan, P. Forrest, P. G. Bannon, and S. M. Grieve. Flow mixing during peripheral veno-arterial extra corporeal membrane oxygenation—a simulation study. *J. Biomech.* 55:64–70, 2017.
[48]Tsai, T. T., M. S. Schlicht, K. Khanafer, J. L. Bull, D. T. Valassis, D. M. Williams, R. Berguer, and K. A. Eagle. Tear size and location impacts false lumen pressure in an ex vivo model of chronic type B aortic dissection. *J. Vasc. Surg.* 47(4):844–851, 2008.
[49]Viggers, R. F., A. R. Wechezak, and L. R. Sauvage. An apparatus to study the response of cultured endothelium to shear stress. *J. Biomech. Eng.* 108(4):332–337, 1986.
[50]Voigt, E. E., C. F. Buchanan, M. N. Rylander, and P. P. Vlachos. Wall shear stress measurements in an arterial flow bioreactor. *Cardiovasc. Eng. Technol.* 3(1):101–111, 2012.
[51]Voyvodic, P. L., D. Min, and A. B. Baker. A multichannel dampened flow system for studies on shear stress-mediated mechanotransduction. *Lab Chip* 12(18):3322–3330, 2012.
[52]White, C. R., H. Y. Stevens, M. Haidekker, and J. A. Frangos. Temporal gradients in shear, but not spatial gradients, stimulate ERK1/2 activation in human endothelial cells. *Am. J. Physiol.-Heart Circ. Physiol.* 289(6):H2350–H2355, 2005.
[53]Wootton, D. M., and D. N. Ku. Fluid mechanics of vascular systems, diseases, and thrombosis. *Annu. Rev. Biomed. Eng.* 1(1):299–329, 1999.
[54]Yamawaki, H., S. Pan, R. T. Lee, and B. C. Berk. Fluid shear stress inhibits vascular inflammation by decreasing thioredoxin-interacting protein in endothelial cells. *J. Clin. Investig.* 115(3):733–738, 2005.
[55]Zeidan, A., S. Javadov, and M. Karmazyn. Essential role of Rho/ROCK-dependent processes and actin dynamics in mediating leptin-induced hypertrophy in rat neonatal ventricular myocytes. *Cardiovasc. Res.* 72(1):101–111, 2006.

[56]Zhang, B., C. Peticone, S. K. Murthy, and M. Radisic. A standalone perfusion platform for drug testing and target validation in micro-vessel networks. *Biomicrofluidics* 7(4):044125, 2013.

[57]Zhu, C., J. H. Seo, and R. Mittal. Computational modelling and analysis of haemodynamics in a simple model of aortic stenosis. *J. Fluid Mech.* 851:23–49, 2018.

[58]Zou, Y., Y. Hu, B. Metzler, and Q. Xu. Signal transduction in arteriosclerosis: mechanical stress activated MAP kinases in vascular smooth muscle cells. *Int. J. Mol. Med.* 1:827–834, 1998.